Low-Voltage Operation AlInN/GaN HEMTs on Si with High Output Power at sub-6 GHz

Katsuhiko Takeuchi[1], Kunihiko Saruta, Shinya Morita, Katsuji Matsumoto, Masashi Yanagita, Satoshi Taniguchi, Shinichi Wada, Kunihiko Tasai, Masayuki Shimada, Katsunori Yanashima
Analog LSI Business Division, Sony Semiconductor Solutions Corporation, Japan
[1]Katsuhiko.Takeuchi@sony.com

***Abstract*—This paper describes the DC and RF performance of AlInN/GaN HEMTs on Si substrates for low-voltage operation to meet the demand of user equipment. By adapting the regrowth ohmic structure, low on-resistance of 0.6 Ω-mm was achieved due to the reduction of the contact resistance. Even with the relatively long gate length of 0.3 µm, lower voltage operation was achieved compared to other reported work. The obtained f_{max} of 53.8 GHz exceeds the requirements of 5G mobile communication applications for the sub-6 GHz frequency range. Large-signal measurements on a gate width of 10x100 µm device exhibited a saturated power density of 1.52 W/mm and power added efficiency of 62.7 % at 5 GHz biased at V_{ds} of 5 V. The device also exhibited excellent performance between V_{ds} of 1.5 V and 12 V. To the best of our knowledge, this represents the highest RF performance with low-voltage operation for a GaN HEMT in the sub-6 GHz region.**

***Keywords*— 5G, power amplifiers, Gallium Nitride, HEMTs.**

I. Introduction

The fifth-generation mobile communication system (5G) has been commercially available since 2019 and is spreading all over the world. Fig. 1 depicts the scope and requirements of the 5G network as defined by the International Telecommunication Union Radiocommunication Sector (ITU-R). In the 5G network, "Enhanced mobile broadband (Enhanced MBB)" enables high speed connections whilst "Low latency, Ultra-reliable" assures extremely low latency, and "Massive machine type communication (Massive MTC)" supports a lot of devices to communicated with each other [1].

5G is implemented in two distinct frequency ranges, the sub-6 GHz region (FR1) and the mm-wave frequencies (FR2). Since power amplifier (PA) operation voltage of the 5G smartphone is typically lower than that of the base station, low voltage operation PAs are needed. So, PAs for 5G smartphone require not only the higher frequency operation compared to fourth-generation mobile communication system (4G) to cover the new FR1 5G bands but also higher peak output powers (*P*out) and higher power added efficiency (PAE) whilst operating at low supply voltages.

GaN-based high-electron-mobility-transistors (HEMTs) are excellent candidates for RF applications such as PA [2]. It is well known that the lattice matched AlInN/GaN HEMTs structure provides a higher two-dimensional electron gas (2DEG) density than AlGaN/GaN structure due to the much stronger spontaneous polarization [3]. Fig. 2(a) shows the band gap energy as a function of the lattice constant and Fig. 2(b) shows 2DEG density as a function of the barrier layer thickness for AlInN and AlGaN. A high 2DEG density contributes to both the increase of drain current and the reduction of knee-voltage, which in turn contributes to a high *P*out and PAE. In addition, the use of a thin barrier layer is effective in reducing the impact of short channel effects especially for shorter gate.

In this work, we demonstrate AlInN/GaN HEMTs on Si substrates for low-voltage operation PAs in sub-6 GHz wireless applications. The highly doped n+-GaN is regrown selectively for source and drain regions to reduce the contact resistance (R_c). Thanks to the low knee-voltage and high breakdown voltage, the obtained RF performances are suitable for sub-6 GHz user equipment PA.

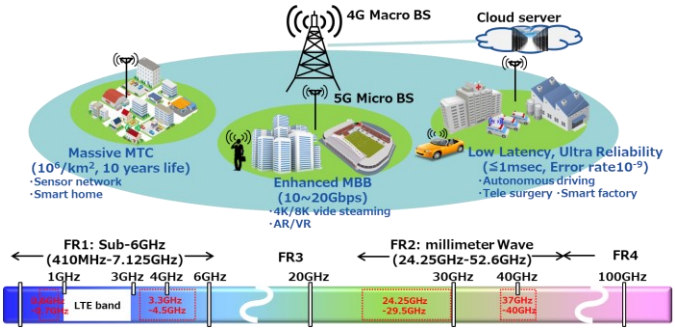

Fig. 1. 5G usage scenarios.

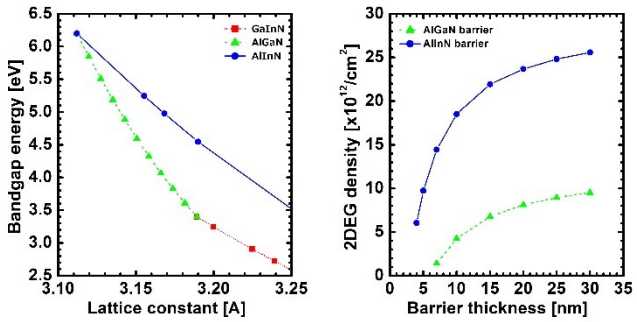

(a) (b)

Fig. 2. Comparison of AlInN and AlGaN (a) the band gap energy as a function of the lattice constant. (b) 2DEG density as a function of the barrier layer thickness.

II. Device Structure

Fig. 3 shows a schematic view of AlInN/GaN HEMTs on Si substrate. The barrier layer is undoped AlInN and the buffer layer is undoped GaN with an AlGaN back barrier. It has a sheet resistance (R_{sh}) of 320 Ω/□, a 2DEG density of 1.5 × 10^{13} cm^{-2} and mobility of 1280 $cm^2/V{\cdot}s$, determined by the Hall measurement.

After the recess etching of the AlInN barrier layer and part of the GaN channel layer for the source and the drain region, ohmic contacts are formed to AlInN/GaN HEMTs by the regrowth of n+-GaN to reduce the R_c between the metal and 2DEG. Silicon nitride (SiN) dielectric is deposited as a passivation layer. After the recess etching of SiN at the gate region, a Ni/Au structure was employed as the gate electrode for creating the Schottky contact.

The transistors have a gate length (L_g) of 0.3 µm, gate-source length (L_{gs}) of 0.5 µm and gate-drain length (L_{gd}) of 0.5 µm, fabricated by i-line stepper.

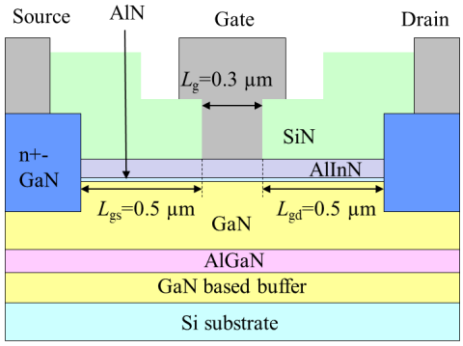

Fig. 3. Schematic cross-sections of the proposed AlInN/GaN HEMT with regrowth of n+-GaN and L_g of 0.3 µm.

III. DC and Pulsed IV Characteristics

Fig. 4 shows the transfer characteristic of a 1x20 µm device at V_{ds} of 5 V. Thanks to the thin barrier thickness of AlInN/GaN HEMTs, a high peak transconductance (g_m) of 0.72 S/mm is realized. As a result of the low R_c, after adapting the regrowth ohmic structure, a low on resistance (R_{on}) of 0.6 Ω-mm is also achieved. A threshold voltage (V_{th}) of -1.6 V at V_{ds} of 5 V is calculated, obtained from linear extrapolation of the drain current.

Fig. 5 shows the I_d–V_{gs} characteristics of a 1x20 µm device at V_{ds} of 5 V for the reference process and improved gate process. Generally, AlInN/GaN Schottky contacts suffer from the larger reverse leakage current than that for AlGaN/GaN due to both the epi quality and the effects of process damage [4]. By altering our gate fabrication to reduce process damage, we have managed to achieve a drain leakage current of < 1x10^{-6} A/mm in our latest device due to the reduction of the gate leakage current. This work is still ongoing and the complete results will be reported in the future.

Fig. 6 shows the pulsed I_d–V_{ds} characteristics of a 10x100 µm device determined by the double pulsing technique. To evaluate the so called "current collapse" which is commonly attributed to GaN device, quiescent bias points of (V_{gq}, V_{dq}) = (0 V to -5 V, 0V to 15 V) were set to evaluate the dynamic knee-voltage and current collapse. It is generally considered that the current collapse in GaN HEMTs is attributed to the electron traps in semiconductor and/or at the interface [5], [6] and can greatly degrade the large-signal characteristics of the device. As our device shows relatively low current collapse for the pulsed IV characteristics, the effect of traps seems sufficiently small for our target application.

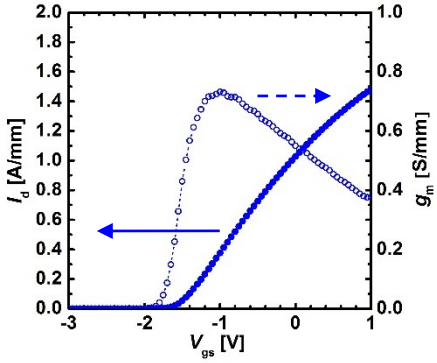

Fig. 4. Transfer characteristics at V_{ds} of 5 V for gate width of 1 x 20 µm.

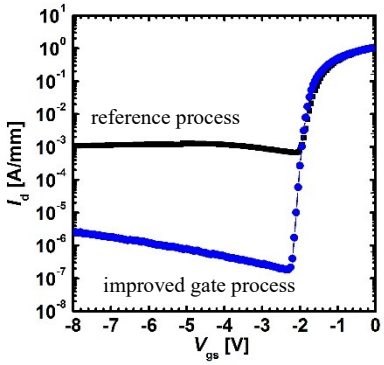

Fig. 5. I_d–V_{gs} characteristics at V_{ds} of 5 V for gate width of 1 x 20 µm.

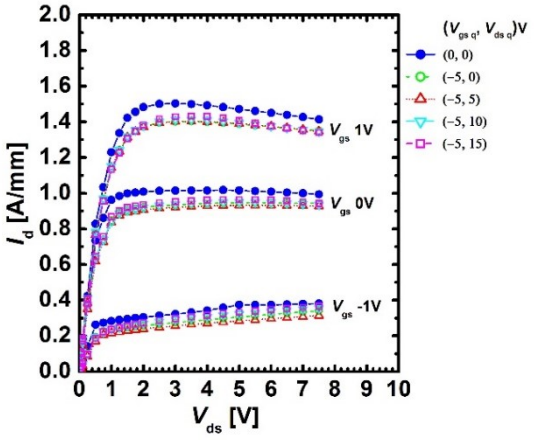

Fig. 6. The pulsed I_d–V_{ds} characteristics at V_{gs} of 1, 0, -1 V for gate width of 10 x 100 µm under various quiescent pulse conditions.

IV. Small-Signal Characteristics

S-parameters were measured in the frequency range of 0.25 to 50 GHz calibrated with an Impedance Standard Substrate (ISS) and results were de-embedded to the device plane with an on-wafer open/short standard. By extrapolating of the short circuit current gain(|H21|) and the maximum stable gain/maximum available gain (MSG/MAG) curves using -20 dB/decade slopes, f_t/f_{max} values of 30.4 / 53.8 GHz are obtained, as shown in Fig. 7. This frequency performance exceeds the requirements for the intended sub-6 GHz applications.

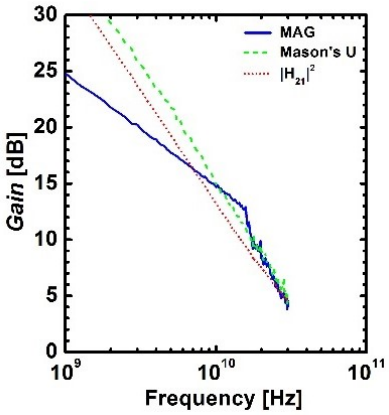

Fig. 7. RF gain characteristics at V_{ds} of 5 V and I_{ds} of 0.1 A/mm for gate width of 10 x 100 µm.

V. Large-Signal Characteristics

The low voltage RF power capability characterizations of AlInN/GaN HEMTs at 5 GHz were carried out in pulsed mode using 2nd/3rd harmonic controlled on-wafer load-pull system. Fig. 8 shows the P_{out}, the power gain (G_t), and the PAE as a function of the input power biased at class AB operation. The load impedance was tuned for the maximum P_{out}. P_d of 1.52 W/mm is achieved for AlInN/GaN HEMTs biased at V_{ds} of 5 V and I_{ds} of 0.1 A/mm.

Fig. 9 shows the P_d and PAE as a function of V_{ds}. The load impedance of P_d, under the corresponding optimum loads. The P_d increases almost linearly with the drain voltage, benefiting from increased drain voltage dynamic range whilst PAE remains constant above 5 V. P_d of 2.66 W/mm and 4.23 W/mm were achieved at V_{ds} of 8 V and 12 V, respectively with > 60 % PAE. The characteristics over V_{ds} confirm the small impact of trapping on large-signal performance, as expected from the results reported in section III.

A performance comparison of our AlInN/GaN HEMTs with previous state of the art results for low voltage operation HEMTs is summarized in Table 1. Thanks to lower knee-voltage and higher I_{ds}, higher P_d is achieved despite the relatively larger L_g of 0.3 µm.

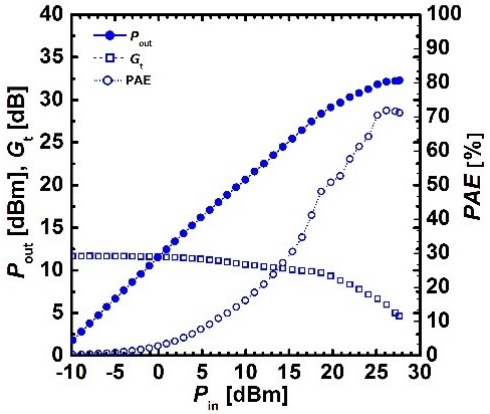

Fig. 8. Large-signal characteristics at 5 GHz biased at V_{ds} of 5 V and I_{ds} of 0.1 A/mm for gate width of 10 x 100 µm under optimum P_{out} load.

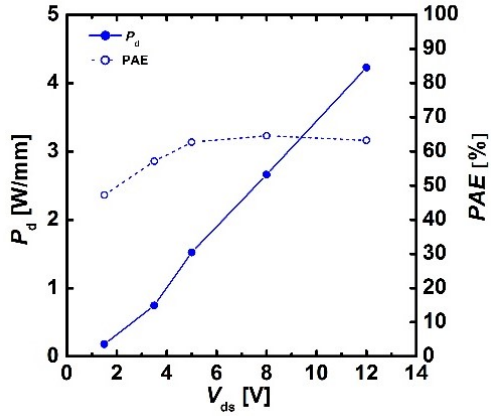

Fig. 9. Large-signal characteristics at P5dB compression as a function of V_{ds} at I_{ds} of 0.1 A/mm obtained from the active load-pull characterization at 5 GHz for gate width of 10 x 100 µm.

Table. 1 Comparison with P_d for low voltage operation HEMTs.

Ref.	L_g [µm]	W_g [mm]	frequency [GHz]	V_d [V]	P_d [W/mm]
[7]	0.2	0.1	8	9	1.6
				15	2.4
[8]	0.09	0.2	6	10	2.3
				15	3.4
	0.19			10	2.1
				15	3.0
[9]	0.09	0.08	28	5	1.5
[10]	0.1	0.2	34	10	2.8
[11]	0.04	-	26.5-40	12	2.3
				14	2.7
[12]	0.15	0.1	30	6	1.2
this work	0.3	1	5	5	1.5
				8	2.7
				12	4.2

VI. Conclusion

In this paper, the DC and RF performance of our low voltage AlInN/GaN HEMTs on Si substrates is presented. DC and pulsed-IV characteristics highlight the relatively small effect of traps on the device performance whilst demonstrating the excellent on-state performance. A best-in-class low voltage power density of 1.52 W/mm and PAE of 62.7 % at a bias voltage of 5 V was obtained from the load-pull measurement at 5 GHz. The device shows excellent performance over a supply range from 1.5 V up to 12 V thanks to the low knee-voltage, high breakdown and low trapping effects. This high RF performance is ideally suited to low-voltage operation power amplifiers for the user equipment in the sub-6 GHz frequency range. Furthermore, the fact that this performance was obtained using silicon substrates, permits the economies of wafer scale required for high volume applications.

Acknowledgment

A part of this work was conducted at NIMS Open Facility of National Institute for Materials Science.

References

[1] "IMT vision—Framework and overall objectives of the future development of IMT for 2020 and beyond," International Telecommunication Union, Geneva, Switzerland, Recommendation ITU-R M.2083, Sep. 2015.

[2] J. Kuzmik. et al., "Power electronics on InAlN/(In)GaN: Prospect for a record performance" *IEEE Electron Device Lett.*, vol. 22, no. 11, pp. 510–512, Nov. 2001.

[3] Meneghini, M. et al., "GaN-based power devices: Physics, reliability, and perspectives" *Journal of Applied Physics*, 130, 181101, Nov. 2021.

[4] Kotani, Junji, et al. "Direct observation of nanometer‐scale gate leakage paths in AlGaN/GaN and InAlN/AlN/GaN HEMT structures." physica status solidi (a) 213.4 (2016): 883-888.

[5] Q. Ma. et al., "InAlN/GaN and AlGaN/GaN HEMT technologies comparison for microwave applications." *Electronics Letters*, vol. 57, issue 15, pp. 591–593, May. 2021.

[6] Velikovskiy, L. E. et al., "Dynamic characteristics after bias stress of GaN HEMTs with field plate on free-standing GaN substrate" *IOP Conference Series: Materials Science and Engineering*, vol. 1019, no. 1, pp. 012071, 2021.

[7] Zhou, Y. et al., "Analysis of Low Voltage RF Power Capability on AlGaN/GaN and InAlN/GaN HEMTs for Terminal Applications" *IEEE Journal of the Electron Devices Society*, vol. 9, pp. 756-762 Aug. 2021.

[8] ElKashlan, R. et al., "Channel Thickness Impact on the Small-and Large-Signal RF Performance of GaN HEMTs on Si with a cGaN Back-Barrier" *IEEE MTT-S International Microwave Symposium*, pp. 910-913 Jun. 2022.

[9] Then, H. W. et al., "Advances in Research on 300mm gallium nitride-on-Si (111) NMOS transistor and silicon CMOS integration" *2020 IEEE International Electron Devices Meeting,* Dec. 2022.

[10] Wang, W. et al "Improvement of power performance of GaN HEMT by using quaternary InAlGaN barrier" *IEEE Journal of the Electron Devices Society*, vol. 6, pp. 360-364, Feb. 2018.

[11] Siddiqi, G. et al., "Improving manufacturability of highly scaled RF GaN HEMTs" *2022 International Conference on Compound Semiconductor Manufacturing Technology,* May. 2022.

[12] Zhou, Y. et al., "High performance millimeter-wave InAlN/GaN HEMT for low voltage RF applications via regrown Ohmic contact with contact ledge structure" *Applied Physics Letters*, 120, 062104, Nov. 2022.